ARTICLE IN PRESS

Available online at www.sciencedirect.com
ScienceDirect
Superlattices and Microstructures ▮ (▮▮▮▮) ▮▮▮–▮▮▮
Superlattices and Microstructures
www.elsevier.com/locate/superlattices

Effects of time reversal symmetry on phonons in sapphire substrate for ZnO and GaN

H.W. Kunert[a,b,*], A. Hoffmann[a], A.G.J. Machatine[b], J. Malherbe[b], J. Barnas[c], G. Kaczmarczyk[a], U. Haboeck[a], R. Seguin[a]

[a] *Institut für Festkörperphysik, Technische Universität Berlin, Hardenbergstr. 36, 10 623 Berlin, Germany*
[b] *Department of Physics, University of Pretoria, Pretoria 0002, South Africa*
[c] *Department of Physics, Adam Mickiewicz University, ul. Umultowska 85, 61-614 Poznan, Poland*

Abstract

Vibrational states in a crystal are classified according to the irreducible representations (irreps) of the corresponding factor group $G_0^{\mathbf{k}}/T$. The wave vector $\mathbf{k}$ runs over the entire Brillouin zone (BZ). For trigonal BZs, the factor groups are determined by the symmetry points Γ, F, L, T, and the symmetry lines Λ, Σ, Y. When the irreps are complex, the time reversal symmetry has to be taken into account. Using the Frobenuis–Schur criterion adapted to space groups with real and complex irreps, we have investigated high symmetry points and lines of the phonons in trigonal crystals: Cr_2O_3, Fe_2O_3, Ti_2O_3, V_2O_3, $FeCO_3$, $CaCO_3$, $CdCO_3$, $MgCO_3$, $MnCO_3$, $NaCO_3$ and $ZnCO_3$, with the common space group $D_{3d}^6(R\bar{3}c)$. We have found several phonons which are influenced by the time reversal symmetry. Therefore, an extra degeneracy of phonons arises. The theoretical results are also compared with available experimental data.

Keywords: Space group theory; Phonons; Semiconductors

1. Introduction

Sapphire (Al_2O_3) is a very common material on the Earth's crust, that crystallizes in the trigonal space group $D_{3d}^6(R\bar{3}c)$. The excellent mechanical and optical properties of the sapphire

* Corresponding author at: Department of Physics, University of Pretoria, 0002 Pretoria, South Africa.
E-mail address: hkunert@nsnper1.up.ac.za (H.W. Kunert).

0749-6036/$ - see front matter © 2007 Published by Elsevier Ltd
doi:10.1016/j.spmi.2007.04.079

make it as a material of choice for various physical and technological applications in its pure and doped forms. It is frequently used as a substrate for growing thin films of such semiconductors, like GaN, ZnO, ZnSe, BeO, 2H-SiC, 4H-SiC, 6H-SiC, MgTe (C_{6v}^4-space group).

Since the sapphire can be easily doped, high Debye frequency and mechanical isotropy studies are undertaken in order to understand its vibrational and electronic states. Sapphire lattice dynamics is poorly understood and is usually studied in the context of phenomenological models adjusted to optical and neutron scattering data. The knowledge of phonons and their symmetries (degeneracies) throughout the BZ strongly facilitates analysis of the experimental and theoretical data on various quasi-particles, as well as interpretation of transport phenomena in the crystal. When a system under consideration is invariant with respect to the time reversal symmetry (TRS), it is possible to regard it as having the symmetry of a nonunitary group which includes the time reversal (TR) operator, in addition to the unitary symmetry operations. The main aim of this paper is to analyse the representations (reps) of such nonunitary groups and to examine the additional degeneracy due to TRS.

The scope of the paper is as follows: in Section 2 we investigate the effects of TRS on vibrational modes. In Section 3 we derive the so-called Lattice Mode Representation (LMR) for sapphire, as well as the connectivity relations throughout the whole BZ, which results in an appropriate phonon assignments at high symmetry points and lines for sapphire. In Section 4 we discuss our results in terms of available experimental data. Section 5 includes brief discussion of the optical selections rules in the presence of TRS, whereas final conclusions are presented in Section 6.

2. Time reversal symmetry in sapphire

Consider the time-dependent Schrödinger equation, $-i\hbar\partial\Psi/\partial t = H\Phi = E\Phi$. Applying the complex conjugate operator and changing t to $-t$ (H: real), one finds $-i\hbar\partial\Psi^*/\partial(-t) = H\Psi^* = E\Psi^*$, which clearly shows that Ψ^* is also an eigenfunction of H. The basis for a representation are now Ψ and Ψ^*, so the dimension of irrps built up on (Ψ, Ψ^*) becomes doubled. Consequently, an extra degeneracy of the states can arise. In the case of TRS, the irreps are complex. Then it is sufficient to find out which irrps of a given group are complex. The criterion for real and complex representations is given by Frobenuis–Schur theorem [1]. Using this theorem we have found the following complex irrps of the D_{3d}^6 group of Al_2O_3: $\Lambda_{1,2,3}$, $P_{1,2,3}$ and $T_{1,2,3}$ for phonons classified according to the single-valued (SV) representations [2]. In addition, we have also investigated spinor or double-valued (DV) representations for optical selection rules. In Table 1 we list the investigated real and complex irrps of saphire.

3. Determination of the possible vibrational modes in Al_2O_3 with D_{3d}^6 space group at $k = 0$ of the first Brillouin zone

In order to derive the LMR [3], we have introduced twenty seven real basis vectors — three displacement and twenty-four angles shown in Fig. 1.

The angles in the Fig. 1 are defined for the lower pyramid as follows: $\alpha_1(312)$; $\alpha_2(123)$; $\alpha_3(231)$; $\beta_1(412)$, $\beta_2(423)$, $\beta_3(431)$, $\beta_4(421)$, $\beta_5(432)$, $\beta_6(413)$; $\delta_1(140)$; $\delta_2(240)$; $\delta_3(340)$. The numbers refer to the ions that make angle in a clockwise manner. The displacements of oxygen ions are: (1) d_1, (2) d_2 and (3) d_3. Similarly, we define the angles for the upper pyramid (primed). The upper ions are obtained through inversion at central aluminum atom, labelled with $4 = 4'$.

The displacements and angles corresponding to the upper (primed) and lower (unprimed) pyramids are related as follows: $d_1 = -d_1'$; $d_2 = -d_2'$; $d_3 = -d_3'$; $\alpha_1(312) =$

Please cite this article in press as: H.W. Kunert, et al., Effects of time reversal symmetry on phonons in sapphire substrate for ZnO and GaN, Superlattices and Microstructures (2007), doi:10.1016/j.spmi.2007.04.079

Table 1
Real and complex representations of D_{3d}^6

High symmetry point and lines	Real and single-valued (SV) representations	Complex representations (spinors). Double-valued (DV) representations
Γ	$\Gamma_{1\pm,2\pm,3\pm}$	$\Gamma_{4\pm,5\pm,6\pm}$(DV)
Λ		$\Lambda_{1,2,3}$(SV)
		$\Lambda_{4,5,6}$(DV)
T		$T_{1,2,3}$(SV)
		$T_{4,5,6}$(DV)
F	$F_{1\pm,2\pm}$	$F_{3\pm,4\pm}$(DV)
L	L_1	L_2(DV)
P		$P_{1,2,3}$(SV)
Σ	$\Sigma_{1,2}$	$\Sigma_{3,4}$(DV)
Y	$Y_{1,2}$	$Y_{3,4}$(DV)

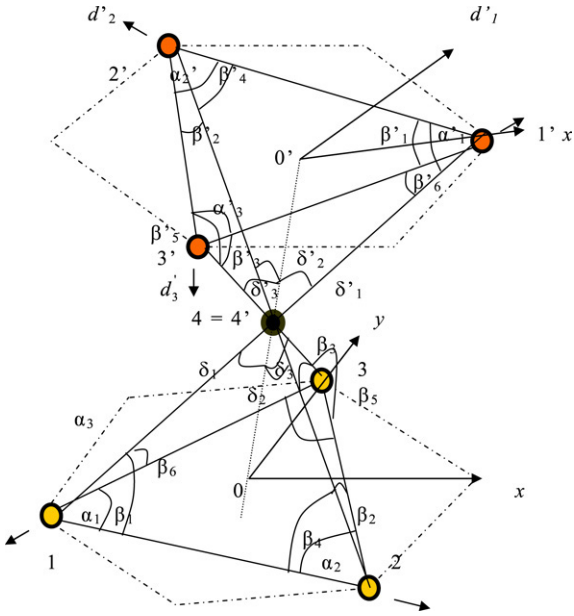

Fig. 1. Arrangement of O and Al atoms in Al_2O_3.

$\alpha_1'(3'1'2') \ldots\ldots\ldots\ldots\ldots \delta_3(340) = \delta_3'(3'4'0')$. The angles of primed coordinates are equivalent to the angles of nonprimed coordinates. Acting by the three generators on the introduced basis we obtain three generating matrices, which form the LMR. For the first generator one finds

$$\{C_3^+|0\}\begin{bmatrix} d_1 \\ d_2 \\ \vdots \\ \vdots \\ \delta_3' \end{bmatrix} = A \begin{bmatrix} d_1 \\ d_2 \\ \vdots \\ \vdots \\ \delta_3' \end{bmatrix}$$

Please cite this article in press as: H.W. Kunert, et al., Effects of time reversal symmetry on phonons in sapphire substrate for ZnO and GaN, Superlattices and Microstructures (2007), doi:10.1016/j.spmi.2007.04.079

where

$$A = D(\{C_3^+ \mid 0\})$$
$$= \lfloor d_2\, d_3\, d_1\, \alpha_2\, \alpha_3\, \alpha_1\, \beta_2\, \beta_3\, \beta_1\, \beta_5\, \beta_6\, \beta_4\, \delta_2\, \delta_3\, \delta_1\, \alpha_2'\, \alpha_3'\, \alpha_1'\, \beta_2'\, \beta_3'\, \beta_1'\, \beta_5'\, \beta_6'\, \beta_4'\, \delta_2'\, \delta_3'\, \delta_1' \rfloor.$$

Here, A is a block-diagonal matrix,

$$A = \begin{bmatrix} A_1 & & \\ & \ddots & \\ & & A_9 \end{bmatrix}, \quad \text{with the sub-matrix } A_i = \begin{bmatrix} 0 & 1 & 0 \\ 0 & 0 & 1 \\ 1 & 0 & 0 \end{bmatrix}$$

for $i = 1, \ldots, 9$. For the second generator associated with nonprimitive translations we have

$$\left\{\sigma_{v1} \mid 00\frac{1}{2}\right\} \begin{bmatrix} d_1 \\ d_2 \\ \vdots \\ \vdots \\ \delta_3' \end{bmatrix} = B \begin{bmatrix} d_1 \\ d_2 \\ \vdots \\ \vdots \\ \delta_3' \end{bmatrix},$$

where

$$B = D\left(\left\{\sigma_{v1} \mid 00\frac{1}{2}\right\}\right)$$
$$= \lfloor d_2\, d_3\, d_1\, \alpha_2\, \alpha_3\, \alpha_1\, \beta_2\, \beta_3\, \beta_1\, \beta_5\, \beta_6\, \beta_4\, \delta_2\, \delta_3\, \delta_1\, \alpha_2'\, \alpha_3'\, \alpha_1'\, \beta_2'\, \beta_3'\, \beta_1'\, \beta_5'\, \beta_6'\, \beta_4'\, \delta_2'\, \delta_3'\, \delta_1' \rfloor$$

and for the rotational generator we get

$$\left\{C_2 \mid 00\frac{1}{2}\right\} \begin{bmatrix} d_1 \\ d_2 \\ \vdots \\ \vdots \\ \delta_3' \end{bmatrix} = C \begin{bmatrix} d_1 \\ d_2 \\ \vdots \\ \vdots \\ \delta_3' \end{bmatrix},$$

with

$$C = D\left(\left\{C_2 \mid 00\frac{1}{2}\right\}\right)$$
$$= \lfloor d_2\, d_3\, d_1\, \alpha_2\, \alpha_3\, \alpha_1\, \beta_2\, \beta_3\, \beta_1\, \beta_5\, \beta_6\, \beta_4\, \delta_2\, \delta_3\, \delta_1\, \alpha_2'\, \alpha_3'\, \alpha_1'\, \beta_2'\, \beta_3'\, \beta_1'\, \beta_5'\, \beta_6'\, \beta_4'\, \delta_2'\, \delta_3'\, \delta_1' \rfloor.$$

By means of the multiplication table we obtain all the other nine matrices of LMR for sapphire. The characters of the LMR together with the characters of irrps (at $\mathbf{k} = 0$) [4] of Al_2O_3 are given in Table 2.

Decomposing the LMR onto irrps listed in Table 1, we obtain the total number of first noninteracting modes and their symmetries (irrps) at $\mathbf{k} = 0$. From the reduction formula [5]:

$$a_\mu = \frac{1}{\|g\|} \sum_\mu \chi^{\mathrm{LMR}}(\{g \mid \tau\}) \cdot \chi_\mu^*(\{g \mid \tau\}), \tag{1}$$

where μ runs over irrps $\Gamma_{1\pm}$, $\Gamma_{2\pm}$, $\Gamma_{3\pm}$ (for $\mathbf{k} = 0$), and $F_{1\pm,2\pm}$, $\Sigma_{1,2}$, $Y_{1,2}$, L_1 (for $\mathbf{k} \neq \mathbf{0}$), we obtain the number of allowed modes, their symmetries, and their degeneracy's spanned by

Please cite this article in press as: H.W. Kunert, et al., Effects of time reversal symmetry on phonons in sapphire substrate for ZnO and GaN, Superlattices and Microstructures (2007), doi:10.1016/j.spmi.2007.04.079

Table 2
Characters of irreducible representations of D_{3d}^6 (at $\mathbf{k} = 0$) and the reducible lattice modes Representation

$\{g/\tau\}$	E	C_3^+	C_3^-	C_{21}''/τ	C_{23}''/τ	C_{22}''/τ	I	S_6^-	S_6^+	σ_{v1}/τ	σ_{v3}/τ	σ_{v2}/τ
G (CDML)	1	3	5	7.1	9.1	11.1	13	15	17	19.1	21.1	23.1
$\Gamma_{1+}(A_{1g})$	1	1	1	1	1	1	1	1	1	1	1	1
$\Gamma_{2+}(A_{2g})$	1	1	1	−1	−1	−1	1	1	1	−1	−1	−1
$\Gamma_{3+}(E_g)$	2	−1	−1	0	0	0	2	−1	−1	0	0	0
$\Gamma_{1-}(A_{1u})$	1	1	1	1	1	1	−1	−1	−1	−1	−1	−1
$\Gamma_{2-}(A_{2u})$	1	1	1	−1	−1	−1	−1	1	1	1	1	1
$\Gamma_{3-}(E_u)$	2	−1	−1	0	0	0	−2	1	1	0	0	0
$\chi^{\mathrm{LMR}}\{g/\tau\}$	27	0	0	−1	−1	−1	3	0	0	−1	−1	−1

Table 3
Normal modes obtained by LMR at high symmetry points and lines of D_{3d}^6 space group (notation according to Ref. [2])

$\Gamma : 2\Gamma_{1+} \oplus 2\Gamma_{1-} \oplus 3\Gamma_{2+} \oplus 2\Gamma_{2-} \oplus 5\Gamma_{3+} \oplus 4\Gamma_{3-}$
$F : 7F_{1+} \oplus 8F_{2+} \oplus 6F_{1-} \oplus 6F_{2-}$
$\Sigma : 13\Sigma_1 \oplus 14\Sigma_2$
$Y : 13Y_1 \oplus 14Y_2$
$L : 27L_1$

Table 4
Compatibility relations of sapphire

$\Gamma \to F : \Gamma_{1+} \to F_{1+}, \Gamma_{2+} \to F_{2+}, \Gamma_{3+} \to F_{1+} \oplus F_{2+}, \Gamma_{1-} \to F_{2-}, : \Gamma_{1-} \to F_{2+}, \Gamma_{2-} \to F_{2-},$
$\Gamma_{3-} \to F_{2-},$
$\Gamma \to \Lambda : \Gamma_{1+} \to \Lambda_1, \Gamma_{2+} \to \Lambda_2, \Gamma_{3+} \to \Lambda_3, \Gamma_{1-} \to \Lambda_2, \Gamma_{2-} \to \Lambda_1, \Gamma_{3-} \to \Lambda_3$
$\Gamma \to \Sigma : \Gamma_{1+} \to \Sigma_1, \Gamma_{2+} \to \Sigma_2, \Gamma_{3+} \to \Sigma_1 \oplus \Sigma_2, \Gamma_{1-} \to \Sigma_1, \Gamma_{2-} \to \Sigma_2, : \Gamma_{3-} \to \Sigma_1 \oplus \Sigma_2$
$T \to Y : T_1 \to Y_1 \oplus Y_2, T_2 \to Y_1 \oplus Y_2, T_3 \to Y_1 \oplus Y_2$
$T \to L : T_1 \to L_1, T_2 \to L_1, T_3 \to L_1$
$T \to P : T_1 \oplus \to P_1 \oplus P_3 T_1 \to \Lambda_3, T_2 \to P3,$
$L \to Y : 2Y_1 \oplus 2Y_2$
$F \to \Sigma : F_{1+} \to \Sigma_1, F_{2+} \to \Sigma_2, F_{1-} \to \Sigma_1, F_{2-} \to \Sigma_2,$

displacement representation (LMR). The characters of F, Σ, Y, and L can be found in Ref. [2]. The obtained normal modes spanned by LMR are listed in Table 3.

Knowing the number and symmetries of allowed vibrational modes, we are able to assign phonons throughout the entire BZ. Splitting of states at the high symmetry points takes usually place by lowering of symmetry. In other words, when going from the point Γ along the lower symmetry axes (Λ, Σ, etc.) the mode-splitting must appear. Using standard group theoretical technique we have established the so-called compatibility relations between the irrps of high symmetry points and lines. The results are summarized in Table 4.

4. Discussion

In this section we discuss the utilities of our results listed in Tables 1–4. In Table 1 we summarized the real and complex irrps of sapphire. The vibrational modes are classified according to the single-valued (SV) irrps, while electrons in conduction and holes in the valence bands, magnons, etc,... (whenever spin is involved) according to the double-valued (DV) irrps,

Please cite this article in press as: H.W. Kunert, et al., Effects of time reversal symmetry on phonons in sapphire substrate for ZnO and GaN, Superlattices and Microstructures (2007), doi:10.1016/j.spmi.2007.04.079

the latter are used in determination of the optical selection rules (discussed in the next section). From Table 2 the symmetries of phonons and therefore their classification is given. For example, at $\mathbf{k} = \mathbf{0}$ we have six TRS uninfluenced modes, $\Gamma_{1\pm}$, $\Gamma_{2\pm}$, $\Gamma_{3\pm}$, while at the point T there are three fourfold degenerate TRS influenced modes, $T_1 \oplus T_1^*$, $T_2 \oplus T_2^*$ and $T_3 \oplus T_3^*$ (and similarly at the point P). From the Table 3 we read the total number of TRS unaffected modes at high symmetry points and lines.

Table 4 provides compatibilities of phonons at different $\mathbf{k}$'s in the entire BZ. This table can be used for an appropriate phonon assignment. The suitable assignment leads to the correct dimensionality of the dynamic matrices from which phonons dispersion curves can be calculated. For example, from $\Gamma \rightarrow \Lambda$ relation we read four $4\Lambda_1$, four $4\Lambda_2$ and nine $9\Lambda_3$ modes. This results is confirmed theoretically by Heid et al. [6] within the density functional method, and by Kappus [7] and Schober et al. [8] by inelastic neutron scattering technique. However, the authors have not assigned the modes.

5. Optical selections rules in the presence of time reversal symmetry

In this section we only briefly discuss the optical selection rules between the states $D \oplus D^*$, that are TRS affected. Ref. [4] tabulates Kronecker Products (KP) of all irrps of 230 space groups, from which the optical selection rules follow. However, the TRS effect has not been taken into account. In the presence of TRS, the KP reads $(D^{(v)} \oplus D^{(v)^*}) \otimes (D^{(\mu)} \oplus D^{(\mu)^*})$ and the corresponding reduction formula is

$$a_\sigma = \frac{1}{|g|} \sum \chi^{(v \oplus v^*) \otimes (\mu \oplus \mu^*)}(\{g \mid \tau_g\}) \cdot \chi^{\sigma}(\{g \mid \tau_g\}). \tag{2}$$

Derivation of the formula will be given elsewhere.

6. Conclusions

In this paper we have studied a comprehensive phonon assignment in sapphire in the presence of time reversal symmetry. A brief indication of TRS effect on the optical selection rules has also been discussed. Our results listed in Tables 1–4 are valid for a number of compounds as; Al_2O_3, Cr_2O_3, Fe_2O_3, Ti_2O_3, V_2O_3, $FeCO_3$, $CaCO_3$, $CdCO_3$, $MgCO_3$, $MnCO_3$, $NaCO_3$, and $ZnCO_3$ with the space group $D_{3d}^6(R\bar{3}c)$.

References

[1] G. Frobenuis, I. Schur, Berl. Ber. 186 (1906).
[2] S.C. Miller, W.F. Love, Tables of Irreducible Representations of Space Groups and Co-Representations of Magnetic Space Groups, Pruett Press, Boulder, CO, 1967.
[3] H.W. Kunert, Appl. Surf. Sci. 212–213 (2003) 890–896.
[4] A.P. Cracknell, B.L. Davies, S.C. Miller, W.F. Love, Kronecker Product Tables, vol. 4, IFI/Plenum Press, New York, Washington, London, 1979.
[5] H.W. Kunert, Eur. Phys. J. Appl. 27 (2004) 251–254.
[6] R. Heid, D. Strauch, K.P. Bohnen, Phys. Rev. B 61 (2000) 8625.
[7] W. Kappus, Z. Phys. B 21 (1975) 325.
[8] H. Schober, D. Schrauch, B. Dorner, Z. Phys. B: Condens. Matter 92 (1993) 273.

Please cite this article in press as: H.W. Kunert, et al., Effects of time reversal symmetry on phonons in sapphire substrate for ZnO and GaN, Superlattices and Microstructures (2007), doi:10.1016/j.spmi.2007.04.079